Manuscript id ZUMJ-2411-3701
DOI: 10.21608/ZUMJ.2025.339311.3701

ORIGINAL ARTICLE

Potential role of angiotensin converting enzyme/neprilysin inhibitor in Lipopolysaccharide induced acute liver injury in male albino rats (Histological and Immunohistochemical Study)

Mohamed A. Shaheen
Medical Histology and Cell Biology department, Faculty of Medicine, Zagazig University, Zagazig, 44519, Egypt

Corresponding author:
Mohamed A. Shaheen,
Email:
drmohamedshaheen@yahoo.com

Submit Date: 30-11-2024
Accept Date: 11-01-2025

Abstract

Background Acute liver injury, a life-threatening condition, is characterized by oxidative stress, inflammation, and apoptosis with limited effective interventions. This study aimed to investigate the potential use of Sacubitril/valsartan (SAC/VAL) in lipopolysaccharide (LPS)-induced acute liver injury. **Methods** Thirty six adult male albino rats were allocated to 3 groups; control groups received either vehicles or SAC/VAL, LPS group received LPS (10 mg/kg, ip) and LPS+SAC/VAL group received LPS and 3 hours later received SAC/VAL (68 mg/kg, oral). Rats were sacrificed 6 hours following LPS injection. **Results** Rats from LPS group had higher serum tumour necrosis factor-alpha (TNF-α), malondialdehyde (MDA) and liver enzymes (ALT and AST), but lower total antioxidant capacity (TAC) than control groups. Histological examination revealed distorted hepatocytes, congested blood vessels, periportal inflammatory cellular infiltration and increased liver injury score in LPS group compared to control group. Ultrastructurally, hepatocytes from LPS group had heterochromatic nuclei with vacuolated cytoplasm, swollen mitochondria and phagosomes. Treatment with SAC/VAL significantly reversed inflammation and oxidative stress and decreased liver injury score. Moreover, hepatocytes from LPS+SAC/VAL group had euchromatic nuclei with intact nucleoplasm. Immunohistochemical evaluation revealed obvious increases in the expression (number of immunopositive cells/field) of Toll-like receptor-4 (TLR-4) and nuclear factor-kappa B (NF-κB) and increased immunoexpression of pyroptotic inflammasome mediators, namely NOD-like receptor protein 3 (NLRP3), caspase-1 (Cas-1) and interleukin-1 beta (IL-1β) in LPS group. SAC/VAL treatment, however reduced these increments. **Conclusion**, SAC/VAL can hinder sepsis-associated acute liver injury by inhibiting inflammation, oxidative stress, mitochondrial distortion, Kupffer cell hyperactivity and cellular pyroptosis.

Keywords: Liver; ultrastructural changes; pyroptosis; TLR-4; sepsis

INTRODUCTION

Sepsis, an infection-induced systemic inflammatory response condition, is a major complication and the main cause of mortality among intensive care patients and following major surgery. Although its worldwide public health concern, the high incidence and hence increased health burden occur in countries with low and

middle income. WHO estimates suggest 11 million deaths from 48.9 million sepsis cases every year. Moreover, sepsis survivors suffer long-term complications as a result [1, 2]. The incidence of sepsis is strongly related to the cell wall glycolipid component of the gram-negative bacteria known as lipopolysaccharide (LPS). The latter activates an inflammatory response that can affect multiple organs leading to life-threatening organ dysfunction with high morbidity and mortality [3]. Challenge with LPS has been widely used to establish animal models for studying acute organ injury and its potential treatment [4-6]. The inflammatory signalling of LPS is triggered by its interaction with the toll-like receptor 4 (TLR4) which upon activation stimulates nuclear factor-kappa B (NF-κB) and its nuclear translocation which thereafter activates the NOD-like receptor protein 3 (NLRP3) inflammasome. These on consequence induce a kind of programmed cell death known as pyroptosis which ìs mediated by inflammatory caspases, leading to excessive inflammatory damage and cell death [7]. Pyroptosis through the increased expression of the inflammatory caspase [caspase-1 (Cas-1)] activates the release of inflammatory cytokines; namely interleukin-1 beta (IL-1β) and interleukin-18 (IL-18) which are key factors in different inflammatory conditions including acute liver injury [3, 8].

The liver is a highly affected organ by sepsis where liver dysfunction often occurs in early sepsis. Experimental and clinical studies revealed that liver dysfunction is an early sign of sepsis and is considered as a specific independent risk factor for poor outcomes in patients with sepsis. Even without pre-existing liver disease, the liver injury due to sepsis is strongly correlated with unfavourable outcomes and increased mortality in septic patients [9]. The early detection and proper intervention are therefore essential to improve survival rates to some extent.

The current preventive measures and the available non-specific treatment options are not sufficient to control sepsis and related complications [5, 10]. Research is therefore encouraging the exploration of a specific and effective therapeutic intervention for septic liver injury to improve outcomes and control sepsis related mortality. Early control of inflammation may be an option to treat sepsis-related acute liver injury.

Sacubitril/valsartan (SAC/VAL) is a neprilysin inhibitor–angiotensin II receptor blocker. This combination therapy was approved by FDA to treat heart failure. In rats with heart failure with preserved ejection fraction, SAC/VAL attenuated myocardial inflammation [11]. Recently, this combination therapy was reported to improve measures of liver function in hypertensive patients with type 2 diabetes and non-alcoholic fatty liver disease [12] and in heart failure patients with reduced ejection fraction [13]. Different studies proved the role of this combined therapy in different inflammatory conditions resulting in the inhibition of the NLRP3 inflammasome in mice with dextran sulfate-induced colitis [14] and apolipoprotein E-deficiency [15].

The aim of this study is to investigate the possible therapeutic effect of SAC/VAL on LPS-induced acute liver injury in rats focusing on histological structural and ultrastructural changes, in addition to pyroptosis-related immunohistochemical alterations.

METHODS

Animals

Thirty-six adult male albino rats (150 ± 30 g) purchased from the animal facility at the faculty of Veterinary Medicine, Zagazig University, Egypt were used in this study. Rats were housed under constant conditions (temperature 25 ± 3°C and relative humidity 50% with 12 hours light/dark cycle). Rats received standard rodent pellet chow (El-Nasr Co., Egypt) and allowed free access to drinking water. The handling of animals and all animal procedures were carried out according to the guidelines approved by the institutional animal care and use committee at Zagazig University (ZU-IACUC); approval number (ZU-IACUC/3/F/207/2024).

Drugs and chemicals

Lipopolysaccharide (LPS) was purchased from Sigma-Aldrich (Saint Louis, MO, United States). Sacubitril/valsartan (SAC/VAL) under trade name Entresto® was provided by Novartis, Cairo, Egypt. Phenobarbital sodium and other analytical grade chemicals were used.

Acute liver injury rat model

After an overnight fast, LPS (dissolved in saline) was given in a dose of 10 mg/kg intraperitoneal (ip) to induce acute liver injury [4, 16].

Experimental design

After 1 week of acclimatization, rats were randomly divided into 3 groups.

1- The control (C) group: included 24 rats were subdivided into 4 subgroups (n=6 each)

- **Negative control (NC) subgroup**: rats were kept without treatment.
- **Vehicle-1 control subgroup**: rats were given 1 ml saline (a vehicle of LPS), once, ip.
- **Vehicle-2 control subgroup**: rats were given 1 ml saline (a vehicle of LPS) once, ip and 3 hours later they receive 1 ml distilled water (a vehicle of SAC/VAL) orally**.**
- **SAC/VAL control subgroup**: rats were given SAC/VAL dissolved in distilled water (68 mg/kg) by oral gavage at 3 hours duration.

2- The LPS-induced acute liver injury (LPS) group: included 6 rats were injected with LPS (10 mg/kg; ip) [4, 16] and left with no further treatment for 6 hours.

3- The LPS+SAC/VAL group: included 6 rats were injected with LPS (10 mg/kg; ip) and 3 hours later received SAC/VAL (68 mg/kg, orally) [17].

The dose and timing of administration of LPS and SAC/VAL were determined based on a preliminary study and previous literature [4, 17].

Sampling

At the end of the 6 hours duration, rats were anaesthetized using sodium phenobarbital (50 mg/kg; ip) [18]. Blood samples were collected for serum separation by centrifugation (2000 xg for 10 minutes at 4°C). Serum samples were used to measure liver function, inflammation and oxidative stress parameters. Liver was removed and rinsed with ice-cold saline, dried to be processed for light and electron microscopic examination.

Briefly, 1 cm^3 specimens from right lobe of the liver were kept in 10% neutral buffered formalin and processed for hematoxylin and eosin (H & E) staining and immunohistochemical studies. Other small pieces (1mm^3) from liver were kept in a 2.5 % buffered glutaraldehyde in 0.1 M sodium cacodylate buffer (pH 7.2) overnight at 4°C for primary fixation then processed for transmission electron microscopy (TEM).

Biochemical analysis

Inflammation, oxidative stress and liver function

Serum level of tumour necrosis factor-alpha (TNF-α) was measured using ELISA kit (E-EL-R2856) provided by ElabScience, Texas, USA. The production of thiobarbituric acid reactive substances, an indicator of lipid peroxidation expressed as malondialdehyde (MDA), and total antioxidant capacity (TAC) were measured in serum using commercial kits (MD 2529 and TA 2513, respectively) provided by Biodiagnostics, Giza, Egypt following the instructions of manufacturer. Serum alanine aminotransferase (ALT) and aspartate aminotransferase (AST) activities were measured using commercially available spectrum diagnostic kits (Egyptian Co for Biotechnology-Spectrum Diagnostics (S.A.E), Obour city industrial area, Egypt) following the manufacturer's instructions. The samples were analysed at Zagazig University, Faculty of Medicine, Biochemistry Department.

Histological study

Light microscope study

Liver tissue samples fixed in 10% neutral buffered formalin were dehydrated in alcohol and were embedded in paraffin wax. Sections (5 µm) were deparaffinized and stained with:

1- Hematoxylin and Eosin: for routine histological examination [19].

2- Immunohistochemical study: The streptavidin-biotin complex immunoperoxidase system [20] was

used for the detection of TLR4, NF-κB, NLRP3, Cas-1 and IL-1β in liver sections following the manufacturer's instructions. Liver sections (5 µm thick) were deparaffinized and rehydrated. Antigen retrieval (microwave treatment, 10 mmol/L citrate buffer, (pH 6) and endogenous peroxidase blocking (3% hydrogen peroxide) were performed according to standard procedures. To prevent non-specific binding, serum blocking solution (3% bovine serum albumin-Cat No. A9418- Sigma-Aldrich Chemical Company, St. Louis, MO, USA) was used. In a humid chamber, liver sections were incubated overnight at 4°C with the primary antibodies (1:500) for **TLR4** (rabbit polyclonal antibody, Affinity Biosciences, Ohio, USA; AF7017), **NF-κB** (rabbit NF-κB monoclonal antibody, ABclonal Technology, Woburn, MA, USA; A19653), **NLRP3** (rabbit NLRP3 monoclonal antibody, MyBioSource, San Diego, CA, USA; MBS8534011), **Cas-1** (rabbit polyclonal antibody, Affinity Biosciences, Ohio, USA, AF5418) and **IL-1β** (rabbit polyclonal antibody, Affinity Biosciences, Ohio, USA, AF5103)**.** Biotinylated goat anti rabbit IgG (MyBioSource, San Diego, CA, USA, MBS674747) was utilised as a secondary antibody (1:5000). After incubation with secondary antibody for 30 minutes and multiple washing, sections were incubated with the streptavidin biotin peroxidase complex (Cat. No. 85878, Sigma-Aldrich Chemical Company, St. Louis, MO, USA) followed by 3, 30-diaminobenzidine tetrahydrochloride (DAB) to visualize the immunoreaction. Sections were finally counterstained with Mayer's hematoxylin and were dehydrated and mounted. Brown colour denoted a positive immunoreaction. For negative control, instead of the primary antibody, PBS was used [21]. Olympus microscope (C5060-AUD, 5H01155, JAPAN) equipped with digital cameras (Canon PowerShot A620, England, UK) were used to examine and capture images at X400 magnification. All micrographs were provided with a scale bar conferring to calibration.

Transmission electron microscope (TEM)

Following the primary glutaraldehyde fixation, liver samples were post-fixed in 1% osmium tetroxide (in distilled water) then tissue was dehydrated in ascending grades of alcohol, cleared in propylene oxide and was impregnated in resin to make hard capsules. Semi-thin (150 nm) sections were prepared using Leica Ultracut UCT microtome (Leica Microsystems, Germany) and were first stained with toluidine blue and examined by a light microscope to check the quality of the preparation process prior to further processing for ultrathin sections. Ultrathin (80 nm) sections were mounted on copper grid and were double stained with Uranyl acetate and Lead citrate [22]. The stained ultrathin sections were examined at 80 kV and photographed using a JEOL TEM (JEM-1200 EX II Electron Microscope, Jeol Ltd, Tokyo, Japan), at the Electron Microscope Research Facility, Faculty of Science, Ain Shams University, Cairo, Egypt.

Morphometric analysis study

The morphometric analysis was blindly executed using image J software. The number of Kupffer cells was counted at X400 in H and E-stained sections. Moreover, the number of TLR4, NF-κB, NLRP3, Cas-1 and IL-1β immunopositive cells were counted in immunohistochemical-stained sections at X400 magnification [23]. Non-overlapping fields (3-4), from six different paraffin-stained sections from six separate rats in each group, were utilised for a quantitative evaluation.

Scoring of liver injury

The scoring of liver injury was accomplished in H and E-stained sections at X400 magnification into (grades 0-4), where Grade 0 = no pathological alterations, Grade 1 = mild congestion or the presence of distorted hepatocytes, Grade 2 = moderate congestion or distorted hepatocytes, grade 3 = apparent congestion or severely distorted hepatocytes and grade 4 = severe congestion or severely distorted hepatocytes [24].

STATISTIC ANALYSIS

Results were expressed as mean ± standard deviation (SD). Data analysis was conducted using GraphPad prism software package, version 8.0 (GraphPad Software, Inc., United States). One-way analysis of variance (ANOVA) followed by Tukey

post Hoc test were employed to compare between the means of different groups considering $P < 0.05$ as statistically significant [25].

RESULTS

The control subgroups did not differ statistically in all biochemical and morphometric measurements. Similarly, histological examination of the liver sections from the control subgroups showed the same histological pattern without any apparent histological alterations during the whole experiment. So, the results of the negative control subgroup (NC) were nominated as a control group for comparison with other experimental groups.

Effect of SAC/VAL on inflammation, oxidative stress and liver function in LPS-induced acute liver injury

The administration of LPS increased serum TNF-α and MDA, while decreased serum TAC as compared to normal control group ($P<0.001$). The treatment with SAC/VAL markedly decreased TNF-α and MDA, but increased TAC as compared to rats in LPS group ($P<0.01$). Serum ALT and AST activities were markedly increased in the LPS group compared to the normal control group. SAC/VAL decreased these liver enzymes significantly compared to LPS group, $P<0.001$ **(Table 1).**

Table 1: Effect of SAC/VAL on inflammation, oxidative stress and liver function in rats with LPS-induced acute liver injury

Serum parameters	NC	LPS	LPS+SAC/VAL
TNF-α (pg/ml)	19.37 ± 1.85	48.57 ± 2.22*	25.25 ± 4.69[a]
MDA (µmol/l)	12.35 ± 1.12	30.22 ± 2.14*	19.12 ± 2.80[a]
TAC (mmol/l)	2.49 ± 0.42	1.25 ± 0.25*	2.00 ± 0.14[a]
ALT activity (U/l)	29.68 ± 3.29	109.28 ± 10.19*	48.97 ± 8.08[a]
AST activity (U/l)	53.27± 4.05	131.88 ± 8.94*	77.66 ± 7.07[a]

Results are expressed as mean ± SD (n=6). *$P < 0.001$ compared to NC group, [a]$P < 0.001$ compared to LPS group. (NC) normal control group, (LPS) LPS-induced liver injury group and (LPS+SAC/VAL) LPS+SAC/VAL-treated group.

Effect of SAC/VAL on histological changes in rats in LPS-induced acute liver injury

Liver sections (H and E-stained) from control group showed normal histological architecture. Each hepatic lobule was formed of closely arranged cords of hepatocytes radiating from the central vein. The central vein was lined with endothelial cells. The hepatic cords were formed of polygonal hepatocytes with acidophilic cytoplasm containing rounded pale vesicular nuclei. Blood sinusoids with their Kupffer and endothelial cells were observed between hepatocyte cords. The portal area containing branches of the portal vein, hepatic artery and bile ducts were seen. No vascular congestion or lymphocytic infiltration were recorded in either the central or portal areas of the liver **(Fig.1).**

LPS-treated rats were presented with distorted hepatic architecture in the form of asymmetrical and loose layout of hepatic cords. Most hepatocytes seemed vacuolated, ballooned with dark nuclei and deeply acidophilic cytoplasm. Few hepatocytes had pale vesicular nuclei. The central vein appeared congested and dilated with mononuclear phagocytic cells in its lumen. Hepatic blood sinusoids appeared congested and dilated with increased number of Kupffer cells in the perisinusoidal area. The portal area showed dilated congested blood vessels and inflammatory cellular infiltrate **(Fig. 1).** The use of SAC/VAL reduced the liver inflammation-induced by LPS both in the central and portal liver areas. Most of the hepatocytes returned to the ordinary hepatic cords pattern and had pale vesicular nuclei, whilst few hepatocytes appeared with dark nuclei. Less congestion was noted in both the central and portal liver areas. Some mononuclear phagocytic cells were observed in the lumen of central vein. Kupffer cells were reduced in number **(Fig. 1)**.

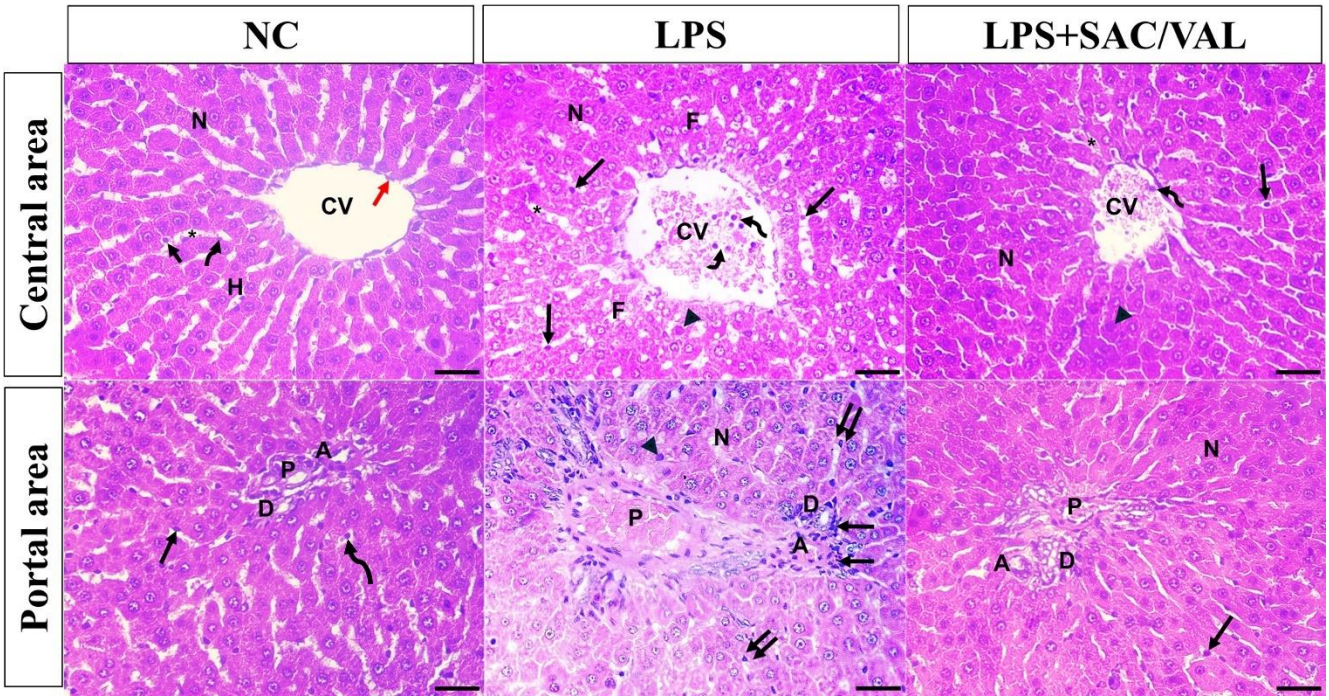

Fig.1 Photomicrographs of H and E stained-paraffin liver sections from different study groups. (NC) Normal control group shows hepatocytes (H) with pale nuclei (N) radiating from the central vein (CV) which is lined with regular flat endothelial cells (red arrow). Hepatic blood sinusoids (Asterix) lie between cords of hepatocytes and are lined with endothelial cells (curved arrow) and Kupffer cells (arrow). The portal area of the control group contains hepatic artery (A), portal vein (P) and bile duct (D). Blood sinusoids are lined by endothelial cells (arrow) and Kupffer cells (curved arrow). No congestion or lymphocytic cellular infiltration are seen. (LPS) LPS group exhibits marked hepatic injury. Most of the hepatocytes have dark nuclei (arrow head) with vacuolations (F). Few hepatocytes have pale nuclei (N). The central vein appears congested and dilated (CV) with mononuclear phagocytic cells in the lumen (curved arrow). Hepatic blood sinusoids seem congested (Asterix) and the distribution of Kupffer cells is augmented (arrow). The portal area of LPS group shows markedly congested portal vein (P) and hepatic artery (A) lymphocytic infiltration (arrow) beside bile duct (D) with increased number of Kupffer cells (double arrow). (LPS+SAC/VAL) LPS+SAC/VAL group is presented with improvement of LPS-related hepatic injury. The central vein (CV) and blood sinusoids (Asterix) show less congestion with few mononuclear phagocytic cells (curved arrow) in the lumen. Most of the hepatocytes appear with pale nuclei (N) whilst few of them have dark nuclei (arrow head). Kupffer cells (arrow) are decreased in number (X400, scale bar 30µm).

Effect of SAC/VAL on immunohistochemical reactivity of TLR4 and NF-κB in rats in LPS-induced acute liver injury

The control group showed a very faint positive cytoplasmic immunoreaction for TLR4 in hepatocytes and a negative immunoreaction for NF-κB. LPS group showed numerous TLR4 positive cells. The reacation is cytoplasmic in hepatocytes, Kupffer cells and mononuclear phagocytic cells in the lumen of the central vein. The immunoreaction of TLR4 was diminished in the cytoplasm of both hepatocytes and Kupffer cells in rats received SAC/VAL treatment**.** Interestingly, LPS administration also showed numerous NF-κB positive cells. The immunoreaction was nuclear both in the hepatocytes and Kupffer cells upon LPS challenge. The use of SAC/VAL decreased the number of NF-κB positive cells. The immunoreaction was nuclear in both hepatocytes and Kupffer cells **(Fig. 2)**.

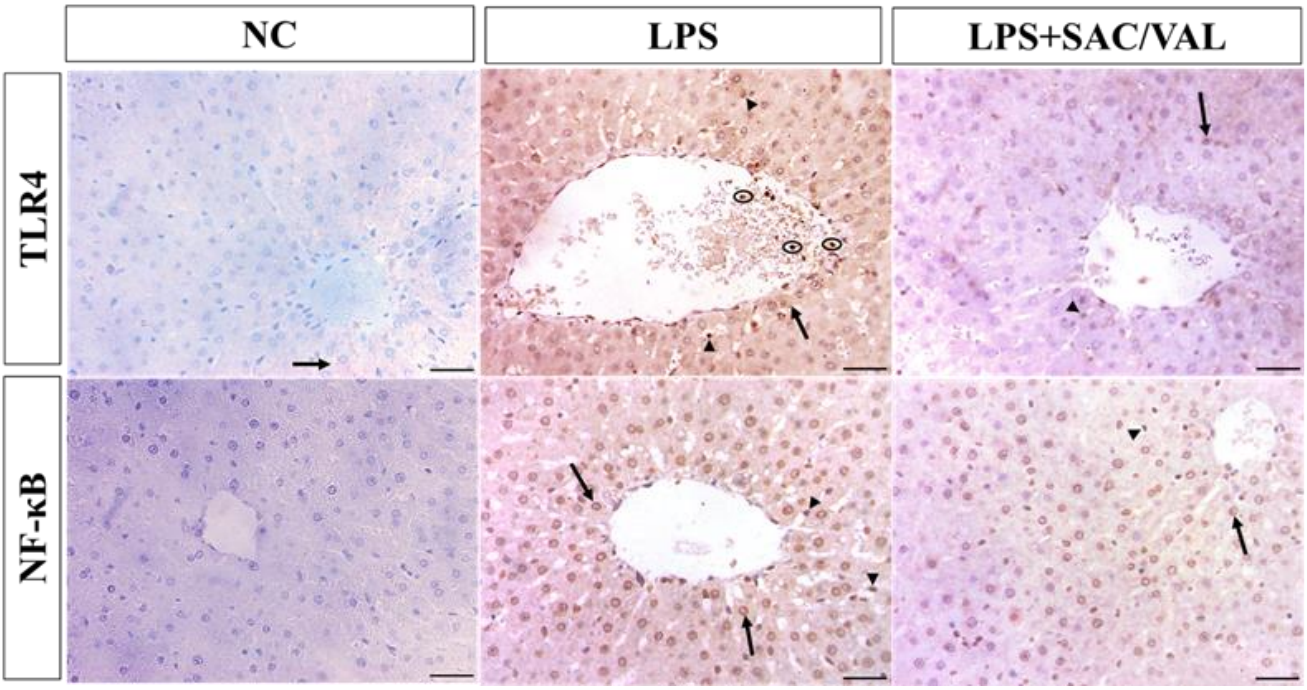

Fig. 2 Photomicrographs of paraffin-stained liver sections for TLR4 and NF-κB immunostaining using the immunoperoxidase reaction. (NC) Normal control group shows a very faint positive immunoreaction for TLR4 in hepatocytes (arrow) and a negative immunoreaction to NF-κB. (LPS) An increased number of TLR4 immunopositive cells is detected in LPS group. The reaction is positive in the cytoplasm of hepatocytes (arrow), Kupffer cells (arrow head) and mononuclear phagocytic cells in the lumen of the central vein (oval). (LPS+SAC/VAL) LPS+SAC/VAL group shows few TLR4 positive cells. The reaction is positive in the cytoplasm of hepatocytes (arrow) and Kupffer (arrow head). Many NF-κB immunopositive cells are seen. The reaction is nuclear in both hepatocytes (arrow) and Kupffer cells of LPS group (arrow head). (LPS+SAC/VAL) Using SAC/VAL resulted in few NF-κB immunopositive positive cells. The reaction is in the nuclei of hepatocytes (arrow) and Kupffer cells (arrow head) (Brown colour indicates a positive reaction, X400, scale bar 30µm).

Effect of SAC/VAL on immunohistochemical reactivity of NLRP3 inflammasome in rats with LPS-induced acute liver injury

To further dissect out the mechanism of LPS-associated liver injury, immunohistochemistry was utilized to look at the reactivity of NLRP3 inflammasome namely via the immunoreaction of NLRP3, Cas-1 and IL-1β cascade. The control groups presented a negative immunoreaction for NLRP3, Cas-1 and a very faint positive cytoplasmic immunoreaction for IL-1β in hepatocytes. The hepatocytes of rats from LPS group that positively express NLRP3, Cas-1 and IL-1β in their cytoplasm were predominant. However, LPS+SAC/VAL group showed few NLRP3, Cas-1 and IL-1β immunopositive hepatocytes. The immunoreaction was cytoplasmic **(Fig. 3).**

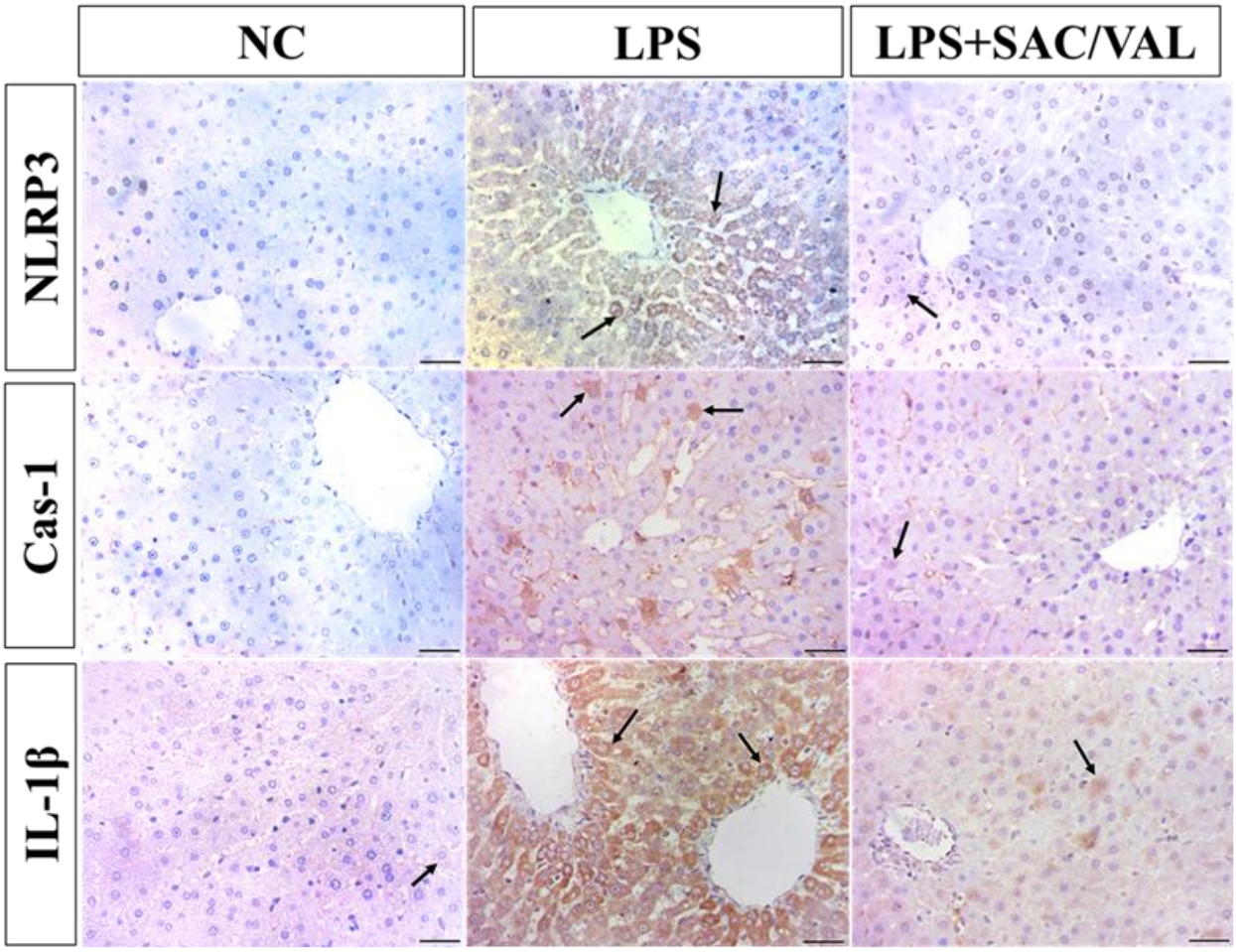

Fig. 3 Immunoperoxidase reaction of paraffin-stained liver sections for NLRP3, Cas-1 and IL-1β immunostaining from different study groups. (NC) Normal Control group exhibits a negative immunoreaction for NLRP3, Cas-1 and a very faint positive immunoreaction for IL-1β in hepatocytes (arrow). (LPS) LPS group shows an increased number of NLRP3, Cas-1 and IL-1β immunopositive hepatocytes. The reaction is cytoplasmic. (LPS+SAC/VAL) LPS+SAC/VAL group displays fewer NLRP3, Cas-1 and IL-1β immunopositive hepatocytes. The reaction is cytoplasmic. Brown colour indicates a positive reaction (arrow) (X400, scale bar 30µm).

Effect of SAC/VAL on the ultrastructure of liver tissue in rats with LPS-induced acute liver injury

The control group liver ultrathin sections revealed normal hepatocytes with euchromatic nuclei and prominent nucleoli. The nuclear envelope seemed intact and regular. The cytoplasm had well developed electron dense mitochondria and rough endoplasmic reticulum with normal cisternae. Bile canaliculi were seen between the neighboring hepatocytes. No vacuolation or pathological alterations were noticed in hepatocytes of the normal control hepatocytes **(Fig 4).**

Normal resting Kupffer cells were seen in the liver blood sinusoids with their characteristic nuclei and their irregular shape with many cytoplasmic extensions. It contained a number of bodies/vacuoles of different shape, density and size. The adjacent hepatocytes exhibited well-

developed mitochondria and they appeared intermingled with Kupffer cells **(Fig 5)**.

LPS group showed a distorted hepatocyte ultrastructure. The nuclei of hepatocytes contained aggregates of irregular coarse heterochromatin with dissolved nucleoplasm. The cytoplasm appears rarified with a swollen distorted rough endoplasmic reticulum and separated cisternae. Mitochondria appeared distorted, swollen, and slightly electron lucent, with loss of their characteristic cristae. Some membrane bound inclusions/vacuoles appeared in the cytoplasm denoting the presence of phagosomes **(Fig 4)**.

Upon LPS challenge, Kupffer cells displayed a marked degree of cellular injury. The cell membrane of the Kupffer cells was lost and the cytoplasm became dissolved. Multiple bodies mostly phagosomes of different sizes and densities were seen in the cytoplasm of the Kupffer cells. The neighbouring hepatocytes had distorted swollen mitochondria and electron lucent vacuoles **(Fig 5)**.

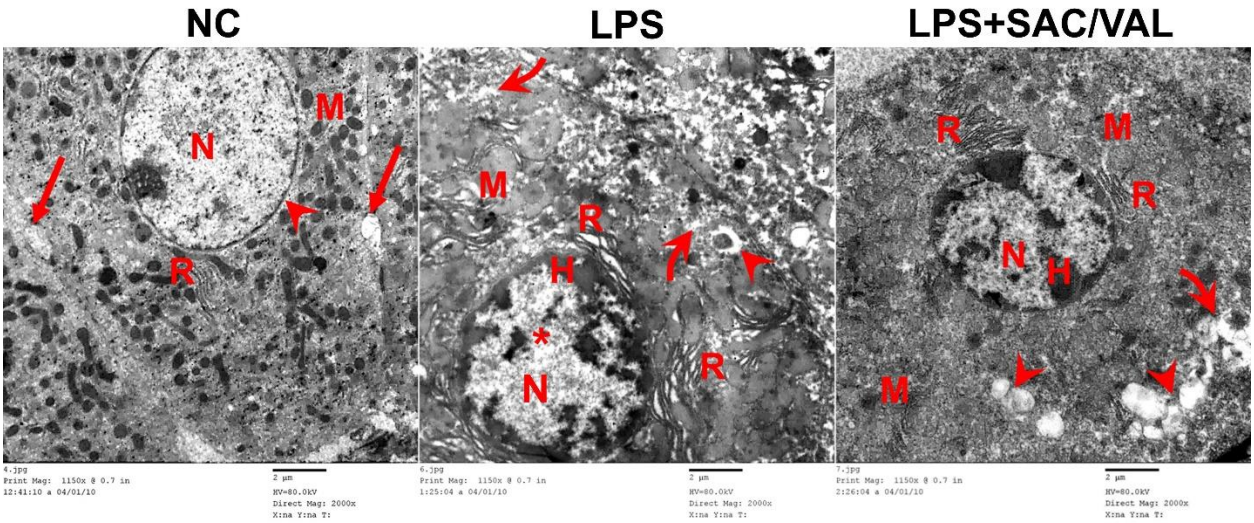

Fig. 4 Transmission electron micrographs of liver specimens from different study groups. (NC) Normal control group shows a hepatocyte with obvious euchromatic nucleus (N). The nuclear envelope appears intact and regular (arrow head). The cytoplasm has well developed electron dense mitochondria (M) and rough endoplasmic reticulum (R) with normal cisternae. Bile canaliculi are seen between the neighboring hepatocytes (arrow). (LPS) LPS group exhibits a distorted hepatocyte. The nucleus (N) contains aggregates of separated irregular coarse heterochromatin (H). The nucleoplasm appears dissolved (Asterix). The cytoplasm appears rarified (curved arrow) with a swollen distorted rough endoplasmic reticulum (R) with separated cisternae. Mitochondria appear distorted, swollen and slightly electron lucent with loss of their characteristics transverse cristae (M). A membrane bound inclusion/vacuole is seen in the cytoplasm (arrow head). (LPS+SAC/VAL) Hepatocytes from LPS+SAC/VAL group exhibit improvement of the histological ultrastructure. The nucleus is mostly euchromatic (N) with intact nucleoplasm. Some heterochromatin is seen in the nucleus (H). The cytoplasm appears with swollen mitochondria with preserved cristae (M) in most of them. The rough endoplasmic reticulum (R) is well developed with preserved cisternae. Electron lucent membrane bound vacuoles of different sizes (arrow head) and a vacuole containing electron dense material (curved arrow) are observed (TEM, X2000, scale bar 2 µm).

Hepatocytes from LPS+SAC/VAL group showed an improvement of the hepatic histological ultrastructure. The nuclei of hepatocytes were mostly euchromatic with intact nucleoplasm however, some heterochromatin was detected in their nuclei. The cytoplasm showed swollen mitochondria with preserved cristae in most of them. The rough endoplasmic reticulum was well-developed with preserved cisternae. Electron lucent membrane bound vacuoles of different sizes and some vacuoles containing electron dense material were elicited **(Fig 4)**.

Kupffer cells from LPS+SAC/VAL group demonstrated an improvement at the ultrastructure level. The Kupffer cell had a regular cell membrane, an intact nucleus and cytoplasm. Multiple membrane bound inclusions/vacuoles of varying densities were seen in the cytoplasm. Electron lucent vacuoles were noticed in the adjacent hepatic parenchymal cells **(Fig 5)**.

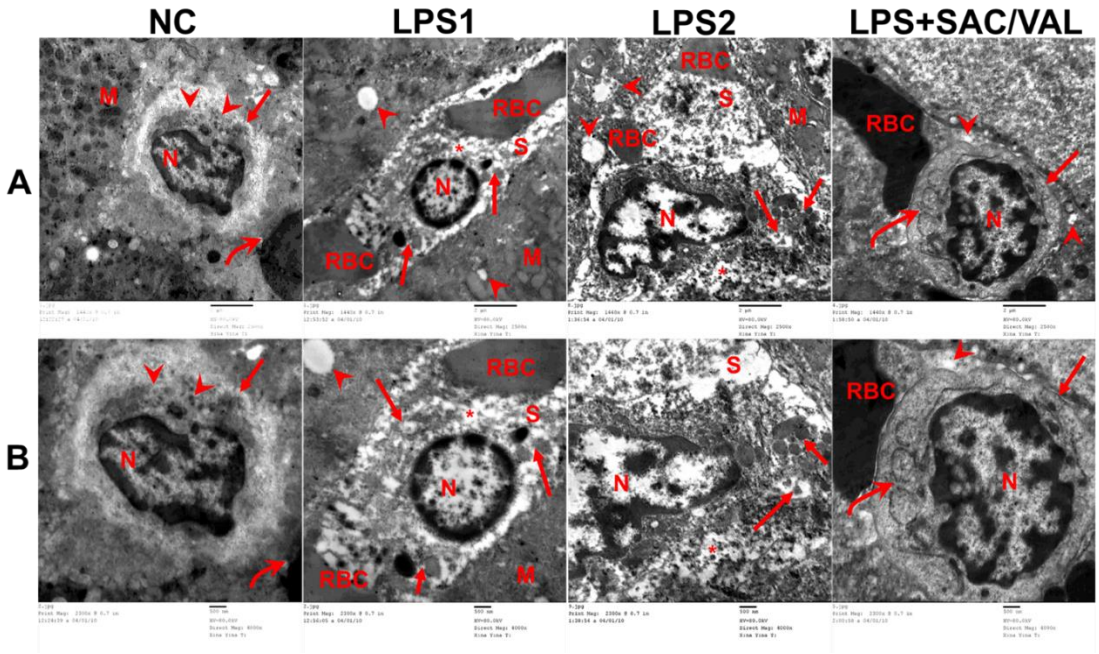

Fig. 5 Ultrastructural changes in Kupffer cells in different study groups. (NC) Normal control group showing a resting Kupffer cell (arrow). It has a characteristic irregular shape and irregular nucleus (N) with many cytoplasmic extensions mostly in a blood sinusoid containing red blood cells (curved arrow). It contains a number of bodies/vacuoles of different shapes, densities and sizes (arrow head). The adjacent hepatocytes appear with well-developed mitochondria (M) and intermingle with the Kupffer cells. (LPS1 and LPS2) Kupffer cells from LPS group are in the lumen of a blood sinusoid (S), containing red blood cells (RBC), with their nuclei (N). The cell membrane of the Kupffer cell is lost (in LPS1) and the cytoplasm is dissolved (Asterix). Multiple bodies mostly phagosomes of different sizes and densities (arrow) are seen in the cytoplasm of the Kupffer cells. The neighbouring hepatocytes have distorted swollen mitochondria (M) and electron lucent vacuoles (arrow head). (LPS+SAC/VAL) LPS+SAC/VAL group showing a Kupffer cell (arrow) in a hepatic blood sinusoid containing red blood cells (RBC). The Kupffer cell has a regular cell membrane, an intact nucleus (N) and cytoplasm. Multiple membrane bound inclusions/vacuoles of varying densities are seen in the cytoplasm (curved arrow). Electron lucent vacuoles are in the adjacent parenchymal cells (arrow head). (A) Kupffer cells from different experimental groups, TEM (X2500, scale bar 2 µm). (B) Kupffer cells from the same groups (same field in A) at higher magnification, TEM (X4000, scale bar 500 nm).

Morphometric results

The number of Kupffer cells was significantly elevated in rats from LPS group (72.72 ± 7.52) compared to control rats (39.06 ± 4.24) and reduced by using SAC/VAL (50.94 ± 7.63) compared to LPS group (P<0.001**).** The number of TLR4, NF-κB, NLRP3, Cas-1 and IL-1β immunopositive cells was significantly higher in rats from LPS group than control rats (P <0.001). However, the number of these positive cells was significantly diminished in LPS+SAC/VAL group as compared to untreated LPS group (P <0.001) **(Table 2).**

Liver injury score

The liver injury score was significantly higher in rats from LPS group than control group littermates (P <0.001). The use of SAC/VAL significantly diminished LPS-associated hepatic damage (P <0.001) as shown in **Table 2**.

Table 2: Effect of SAC/VAL on morphometric parameters and injury score in rats with LPS-induced acute liver injury

	NC	LPS	LPS+SAC/VAL
Kupffer cells (cells/field)	39.06 ± 4.24	72.72 ± 7.52*	50.94 ± 7.63[a]
TLR4 positive cells (cells/field)	0.72 ± 0.57	121.33 ± 12.43	49.94 ± 10.01
NF-κB positive cells (cells/field)	0 ± 0	155.22 ± 22.29	91.06 ± 12.26
NLRP3 positive cells (cells/field)	0 ± 0	142.95 ± 26.99*	1.17 ± 0.92[a]
Cas-1 positive cells (cells/field)	0 ± 0	27.52 ± 5.83*	4.62 ± 2.58[a]
IL-1β positive cells (cells/field)	1.11 ± 0.90	196.28 ± 15.04*	58.39 ± 10.16*
Liver injury score	0 ± 0	3.3 ± 0.57*	1.59 ± 0.41[a]

Results are expressed as mean ± SD (n=6). *P <0.001 compared to NC group, [a]P <0.001 compared to LPS group. (NC) normal control group, (LPS) LPS-induced liver injury group and (LPS+SAC/VAL) LPS+SAC/VAL-treated group.

DISCUSSION

Acute liver injury caused by sepsis is a major health concern with an uncontrollable inflammatory response that arises as early as few hours following exposure to LPS [26]. The need for therapy to effectively manage this condition is therefore essential. In this study we selected the newly combined sacubitril/valsartan therapy (SAC/VAL), an approved FDA drug for the treatment of heart failure, to be tested as a proposed therapy for sepsis-induced acute liver injury and proved its effectiveness using histological and biochemical measurements. In the current study, SAC/VAL showed neutral effects on the normal liver regarding histological and biochemical parameters. Hepatotoxicity of SAC/VAL is very rare, however, one case report showed hepatotoxicity in a 90-year-old female patient with chronic heart failure. She developed an increase in liver enzymes which returned to normal upon withdrawal of SAC/VAL. Advanced age and past history of tuberculous pleurisy were reported as the risk factors for the reported SAC/VAL hepatotoxicity in this female patient [27].

LPS is an accepted common animal model of acute liver injury [4, 28, 29]. LPS is known as a powerful trigger of pro-inflammatory signalling pathways [28]. In the present study, the exposure to LPS initiated an inflammatory response as indicated by increased serum TNF-α which is a pivotal cytokine that exacerbated the production of reactive oxygen species (ROS). In addition, the increased generation of ROS is associated with depletion of antioxidant defense machinery resulting in oxidative stress which are, in part, responsible for liver cell injury [26, 30, 31].

Oxidative stress (increased serum MDA and decreased serum TAC) was apparent 6 hours following LPS exposure. The higher mitochondrial content of hepatocytes, due to their increased requirement of adenosine triphosphate (ATP) than other cells, makes hepatocytes more vulnerable to injury by oxidative stress [32]. As a result, considerable liver injury in rats at 6 hours following the administration of LPS was evident and was indicated by the deterioration in liver function (increased serum ALT and AST activities). These enzymes are essential liver enzymes located in the cytoplasm of hepatocytes. The activity of ALT has been described to be about 3000 times more in hepatocytes than in serum. Augmented serum activity of ALT is present during acute liver insult. Immediately following acute insult of liver injury, serum AST increases, reaching a higher level than ALT. Direct measurement of ALT and AST activity is an efficient and accurate means for assessment of acute liver damage [33]. The increased serum TNF-α, MDA, ALT and AST activities and depleted TAC by LPS are in line with previous studies [26, 34]. Treatment with antioxidant and anti-inflammatory agents were beneficial in LPS-induced liver injury [16]. This study similarly showed that the use of SAC/VAL significantly amended oxidative and inflammatory changes and hence reversed the deterioration of liver enzymes in serum. The anti-inflammatory effects of SAC/VAL was previously reported in myocardial inflammation [11, 35], colitis [14] and apolipoprotein E- deficient atherosclerosis [15]. The improvement of liver function by SAC/VAL was also previously reported in hypertensive patients with type 2 diabetes and non-alcoholic fatty liver disease [12] and in heart failure patients with reduced ejection fraction [13].

The structural architecture of the liver, upon LPS challenge, showed markedly distorted, ballooned, and vacuolated hepatocytes. Activation and increased number of Kupffer cells were also observed along with vascular congestion both in the central and portal veins. Marked infilammatory cellular infiltrate and the liver injury score were also significantly aggravated by LPS challenge. This agrees with what had been observed in previous studies [16, 26].

Deeply acidophilic cytoplasm was also detected in hepatocytes upon LPS challenge. This acidophilic cytoplasm refers to enlarged mitochondria which resulted from inflamed hepatocytes depending on the severity of inflammation as described by Leow et al. [36] The hepatic injury appeared rapidly following the challenge by LPS due to the increased liability of hepatocytes to oxidative damage than other cell types [32].

In the present work, using TEM, mitochondria from LPS group appeared distorted, swollen, and slightly electron lucent, with loss of their characteristic cristae denoting marked cellular and mitochondrial injury. This matches with earlier studies which admitted that mitochondrial injury is an associated feature of cell injury/insult including sepsis [7, 37]. Moreover, the release of mitochondrial DNA from injured hepatocytes may further activate neutrophils leading to worsening of liver injury [37]. These mitochondrial changes are also in part responsible for the uncontrolled ROS production [7].

Ultrastructurally, the cytoplasm of hepatocytes from rats received LPS appeared rarified with distorted and swollen mitochondria. Cytoplasmic vacuolations were also detected and denoting the presence of phagosomes. This is line with Oami et al [38] who showed similar results in a murine sepsis model. Indeed, the presence of phagosomes is a cellular protective mechanism by enhancing the bactericidal activities of the hepatocytes in a response to LPS

challenge to localize E.coli with the autophagosomes [39]. An earlier study was performed by Watanabe and colleagues [40] in a clinical and laboratory-based study who showed that hepatocyte vacuolations were the same in both murine and patients during sepsis.

It is well known that Kupffer cells act as local macrophages in the liver and have an important role during hepatic insult [41]. Results from the current study showed that the number of Kupffer cells was significantly higher in rats from LPS group than normal control littermates. Ultrastructurally, Kupffer cells had vacuoles upon LPS challenge which are characteristic features of active Kupffer cells. This is matched with findings shown by Watanabe et al [40]. In the present study, loss of the cell membrane of the Kupffer cells, using TEM, was noticed. This agrees with results shown by Fan et al., [42]. They reported pyroptosis of Kupffer cells upon LPS challenge, presented as holes and rupture of the cell membrane of Kupffer cells using scanning electron microscopy.

Interestingly, the administration of SAC/VAL alleviated the hepatic inflammation and injury induced by LPS in terms of alleviation of the hepatic congestion, inflammatory cellular infiltration and Kupffer cell activation / injury. Liver injury score was improved, as shown by H and E results, by the administration of SAC/VAL compared to LPS group as well.

The liver injury from sepsis was reported to be linked to pyroptosis, a kind of programmed cell death induced by inflammatory caspases leading to excessive inflammatory damage and cell death [7]. To further elucidate the possible mechanism/pathway of LPS-associated liver injury, immunohistochemical technique was employed to study mediators involved in pyroptosis-induced cell death. The immunoexpression of both TLR4 and NF-κB in liver sections were first investigated. Previous studies have shown that LPS is a crucial TLR4 binding molecule that can induce liver damage through triggering the TLR4/NF-κB signalling pathway [43, 44]. The binding of LPS to TLR4 activated the transcription factor NF-κB and hence its translocation to the nucleus. In the present work, the number of TLR4 and NF-κB immunopositive hepatocytes and Kupffer cells was significantly increased in LPS group compared to the control group. This is in accordance with what has been elucidated by Chen et al [43].

In this study, LPS+SAC/VAL group exhibited a significant decrease in the number of TLR4 and NF-κB immunopositive hepatocytes and Kupffer cells compared to LPS group. In agreement with these results, SAC/VAL was previously repoted to inhibit the activation and the nuclear translocation of NF-κB and thereby attenuated inflammation and cardiomyocyte apoptosis reducing cardiac dysfunction and remodelling in mice with myocardial ischemia/reperfusion injury [35]. Once translocated to the nucleus, NF-κB can stimulate the transcription of NLRP3 [45]. It has been documented that the expression NLRP3 inflammasome gene was augmented in the liver upon exposure to LPS [8, 46]. These findings suggested a crucial role of the NLRP3 inflammasome in LPS-induced inflammation and hereafter hepatic failure. Moreover, the impaired swollen mitochondria and the production of ROS can trigger Cas-1 activation which in turn mediate pyroptosis [7].

In rats exposed to LPS, the increased NLRP3 expression in the cytoplasm of the hepatocytes occurs and this consequently assembles with Cas-1 which activates the NLRP3 inflammasome leading to the cleavage of procytokines and the release of mature cytokines including IL-1β. This occurs via stimulation of pro-IL-1β to form the active IL-1β which

aggravates the inflammatory reaction to recruit the pyroptosis process to start cell lysis [8, 46]. In the current study, the number of NLRP3, Cas-1 and IL-1β hepatic immunopositive cells increased significantly upon LPS challenge compared to the control group. This is in accordance with previous studies [7, 29]. Remarkably, the number of hepatic NLRP3, Cas-1 and IL-1β positive cells decreased significantly in response to LPS challange upon the use of SAC/VAL.

CONCLUSION

The acute hepatic injury induced by LPS involved oxidative stress, inflammation which mediated cellular damage via pyroptosis as confirmed by biochemical, histological, TEM, and immunohistochemistry results. The associated hepatic injury also involved mitochondrial distortion and Kupffer cell hyperactivity/injury. Results from this study provided evidence that SAC/VAL can hinder pyroptosis and prevent sepsis-associated acute liver injury.

REFERENCES

1-Guidelines on the Clinical Management of Sepsis [https://www.who.int/news-room/fact-sheets/detail/sepsis]

2-Rudd KE, Johnson SC, Agesa KM, Shackelford KA, Tsoi D, Kievlan DR, et al. Global, regional, and national sepsis incidence and mortality, 1990-2017: analysis for the Global Burden of Disease Study. Lancet 2020; 395: 200-11.

3-Zheng Y, Gao Y, Zhu W, Bai XG, Qi J. Advances in molecular agents targeting toll-like receptor 4 signaling pathways for potential treatment of sepsis. Eur J Med Chem 2024; 268: 116300.

4-Gao H, Yang T, Chen X, Song Y. Changes of Lipopolysaccharide-Induced Acute Kidney and Liver Injuries in Rats Based on Metabolomics Analysis. J Inflamm Res 2021; 14: 1807-25.

5-Pravda J. Sepsis: Evidence-based pathogenesis and treatment. World J Crit Care Med 2021; 10: 66-80.

6-Zhao Q, Sheng MF, Wang YY, Wang XY, Liu WY, Zhang YY, et al. LncRNA Gm26917 regulates inflammatory response in macrophages by enhancing Annexin A1 ubiquitination in LPS-induced acute liver injury. Front Pharmacol 2022; 13: 975250.

7-Wang PF, Xie K, Cao YX, Zhang A. Hepatoprotective Effect of Mitochondria-Targeted Antioxidant Mito-TEMPO against Lipopolysaccharide-Induced Liver Injury in Mouse. Mediators Inflamm 2022; 2022: 6394199.

8-Chen Y, Ye X, Escames G, Lei W, Zhang X, Li M, et al. The NLRP3 inflammasome: contributions to inflammation-related diseases. Cell Mol Biol Lett 2023; 28: 51.

9-Yan J, Li S, Li S. The role of the liver in sepsis. Int Rev Immunol 2014; 33: 498-510.

10-Evans T. Diagnosis and management of sepsis. Clin Med (Lond) 2018; 18: 146-9.

11-Shi YJ, Yang CG, Qiao WB, Liu YC, Liu SY, Dong GJ. Sacubitril/valsartan attenuates myocardial inflammation, hypertrophy, and fibrosis in rats with heart failure with preserved ejection fraction. Eur J Pharmacol 2023; 961: 176170.

12-Uchimoto S. Effects of Sacubitril/Valsartan on Liver Function in Hypertensive Patients with Type 2 Diabetes. Journal of Clinical Physiology 2024; 54: 37 - 44.

13-Suzuki K, Claggett B, Minamisawa M, Packer M, Zile MR, Rouleau J, et al. Liver function and prognosis, and influence of sacubitril/valsartan in patients with heart failure with reduced ejection fraction. Eur J Heart Fail 2020; 22: 1662-71.

14-Chiu HW, Wu CH, Lin WY, Wong WT, Tsai WC, Hsu HT, et al. The Angiotensin II Receptor Neprilysin Inhibitor LCZ696 Inhibits the NLRP3 Inflammasome By Reducing Mitochondrial Dysfunction in Macrophages

and Alleviates Dextran Sulfate Sodium-induced Colitis in a Mouse Model. Inflammation 2024; 47: 696-717.

15-Zhang H, Liu G, Zhou W, Zhang W, Wang K, Zhang J. Neprilysin Inhibitor-Angiotensin II Receptor Blocker Combination Therapy (Sacubitril/valsartan) Suppresses Atherosclerotic Plaque Formation and Inhibits Inflammation in Apolipoprotein E- Deficient Mice. Sci Rep 2019; 9: 6509.

16-Liu Y, Li F, Zhang L, Wu J, Wang Y, Yu H. Taurine alleviates lipopolysaccharide-induced liver injury by anti-inflammation and antioxidants in rats. Mol Med Rep 2017; 16: 6512-7.

17-Li X, Braza J, Mende U, Choudhary G, Zhang P. Cardioprotective effects of early intervention with sacubitril/valsartan on pressure overloaded rat hearts. Sci Rep 2021; 11: 16542.

18-Oh SS, Narver HL. Mouse and Rat Anesthesia and Analgesia. Curr Protoc 2024; 4: e995.

19-Suvarna SK, Layton C, Bancroft JD: Bancroft's Theory and Practice of Histological Techniques. 8th edition edn. China: Elsevier; 2019.

20-Sanderson T, Wild G, Cull AM, Marston J, Zardin G: Immunohistochemical and immunofluorescent techniques. In Bancroft's Theory and Practice of Histological Techniques. 8th edition edition. Edited by Suvarna SK, Layton C, Bancroft JD. China: Elsevier; 2019: 337-94

21-Ramos-Vara JA, Kiupel M, Baszler T, Bliven L, Brodersen B, Chelack B, et al. Suggested guidelines for immunohistochemical techniques in veterinary diagnostic laboratories. J Vet Diagn Invest 2008; 20: 393-413.

22-Tizro P, Choi C, Khanlou N. Sample Preparation for Transmission Electron Microscopy. Methods Mol Biol 2019; 1897: 417-24.

23-Jensen EC. Quantitative analysis of histological staining and fluorescence using ImageJ. Anat Rec (Hoboken) 2013; 296: 378-81.

24-Ishak K, Baptista A, Bianchi L, Callea F, De Groote J, Gudat F, et al. Histological grading and staging of chronic hepatitis. J Hepatol 1995; 22: 696-9.

25-Mishra P, Singh U, Pandey CM, Mishra P, Pandey G. Application of student's t-test, analysis of variance, and covariance. Ann Card Anaesth 2019; 22: 407-11.

26-Miao F, Geng S, Ning D. Hydroxytyrosol ameliorates LPS-induced acute liver injury (ALI) in mice by modulating the balance between M1/M2 phenotype macrophage and inhibiting TLR4/NF-κB activation. Journal of Functional Foods 2023; 102: 105455.

27-Zhang T, Cai JL, Yu J. Sacubitril/valsartan-induced liver injury: A case report and literature review. Medicine (Baltimore) 2023; 102: e34732.

28-Daniela Benedeto-Stojanov, Vanja P. Ni˘ckovi´c, Gordana Petrovi´c, Andrija Ranci´c, Ivan Grgov, Gordana R. Nikoli´c, et al. Melatonin as a Promising Anti-Inflammatory Agent in an In Vivo Animal Model of Sepsis-Induced Rat Liver Damage. International Journal of Molecular Sciences 2024; 25: 455.

29-Wang G, Jin S, Huang W, Li Y, Wang J, Ling X, et al. LPS-induced macrophage HMGB1-loaded extracellular vesicles trigger hepatocyte pyroptosis by activating the NLRP3 inflammasome. Cell Death Discov 2021; 7: 337.

30-Bhol NK, Bhanjadeo MM, Singh AK, Dash UC, Ojha RR, Majhi S, et al. The interplay between cytokines, inflammation, and antioxidants: mechanistic insights and therapeutic potentials of various antioxidants and anti-cytokine compounds. Biomedicine and Pharmacotherapy 2024; 178: 117177.

31-Zhang Q, Jiang Y, Qin Y, Liu J, Xie Y, Zhang L, et al. Linoleic Acid Alleviates Lipopolysaccharide Induced Acute Liver Injury via Activation of Nrf2. Physiol Res 2024; 73: 381-91.

32-Dwivedi DK, Jena GB. Glibenclamide protects against thioacetamide-induced hepatic damage in Wistar rat: investigation on NLRP3, MMP-2, and stellate cell activation. Naunyn Schmiedebergs Arch Pharmacol 2018; 391: 1257-74.

33-Kim WR, Flamm SL, Di Bisceglie AM, Bodenheimer HC, Public Policy Committee of the American Association for the Study of Liver D. Serum activity of alanine aminotransferase (ALT) as an indicator of health and disease. Hepatology 2008; 47: 1363-70.

34-Doganyigit Z, Okan A, Kaymak E, Pandir D, Silici S. Investigation of protective effects of apilarnil against lipopolysaccharide induced liver injury in rats via TLR 4/ HMGB-1/ NF-kappaB pathway. Biomed Pharmacother 2020; 125: 109967.

35-Xiao F, Wang L, Liu M, Chen M, He H, Jia Z, et al. Sacubitril/valsartan attenuates myocardial ischemia/reperfusion injury via inhibition of the GSK3beta/NF-kappaB pathway in cardiomyocytes. Arch Biochem Biophys 2022; 730: 109415.

36-Leow WQ, Chan AW, Mendoza PGL, Lo R, Yap K, Kim H. Non-alcoholic fatty liver disease: the pathologist's perspective. Clin Mol Hepatol 2023; 29: S302-S18.

37-Liu X, Yu T, Hu Y, Zhang L, Zheng J, Wei X. The molecular mechanism of acute liver injury and inflammatory response induced by Concanavalin A. Mol Biomed 2021; 2: 24.

38-Oami T, Watanabe E, Hatano M, Teratake Y, Fujimura L, Sakamoto A, et al. Blocking Liver Autophagy Accelerates Apoptosis and Mitochondrial Injury in Hepatocytes and Reduces Time to Mortality in a Murine Sepsis Model. Shock 2018; 50: 427-34.

39-Wang J, Feng X, Zeng Y, Fan J, Wu J, Li Z, et al. Lipopolysaccharide (LPS)-induced autophagy is involved in the restriction of Escherichia coli in peritoneal mesothelial cells. BMC Microbiol 2013; 13: 255.

40-Watanabe E, Muenzer JT, Hawkins WG, Davis CG, Dixon DJ, McDunn JE, et al. Sepsis induces extensive autophagic vacuolization in hepatocytes: a clinical and laboratory-based study. Lab Invest 2009; 89: 549-61.

41-Papachristoforou E, Ramachandran P. Macrophages as key regulators of liver health and disease. Int Rev Cell Mol Biol 2022; 368: 143-212.

42-Fan G, Li Y, Chen J, Zong Y, Yang X. DHA/AA alleviates LPS-induced Kupffer cells pyroptosis via GPR120 interaction with NLRP3 to inhibit inflammasome complexes assembly. Cell Death Dis 2021; 12: 73.

43-Chen SN, Tan Y, Xiao XC, Li Q, Wu Q, Peng YY, et al. Deletion of TLR4 attenuates lipopolysaccharide-induced acute liver injury by inhibiting inflammation and apoptosis. Acta Pharmacol Sin 2021; 42: 1610-9.

44-Tang YL, Zhu L, Tao Y, Lu W, Cheng H. Role of targeting TLR4 signaling axis in liver-related diseases. Pathol Res Pract 2023; 244: 154410.

45-Swanson KV, Deng M, Ting JP. The NLRP3 inflammasome: molecular activation and regulation to therapeutics. Nat Rev Immunol 2019; 19: 477-89.

46-Paik S, Kim JK, Silwal P, Sasakawa C, Jo EK. An update on the regulatory mechanisms of NLRP3 inflammasome activation. Cell Mol Immunol 2021; 18: 1141-60.

Citation

Shaheen, M. Potential role of angiotensin converting enzyme/neprilysin inhibitor in Lipopolysaccharide induced acute liver injury in male albino rats (Histological and Immunohistochemical Study). *Zagazig University Medical Journal*, 2025; (416-431): -. doi: 10.21608/zumj.2025.339311.3701